Advanced Electric Systems and Aerodynamics for Efficiency Improvements in Heavy Duty Trucks

Final Report

Contractor: Caterpillar Inc.
Contract No.: DE-FC26-04NT42189

Principal Investigator: Larry M. Slone
Caterpillar Inc. – Technology & Solutions Division
(309) 578-0243, fax: (309) 578-6285, e-mail: slone_larry_m@cat.com

Caterpillar Program Manager: Jeffrey F. Birkel
Caterpillar Inc. – Technology & Solutions Division
(309) 636-1077, fax: (309) 636-2567, e-mail: birkel_jeffrey_f@cat.com

Consortium Team Members:
Engineered Machined Products (EMP)
Switched Reluctance Drives LTD (SRDL), division of Emerson Electric Co.

Project Manager: Ralph D. Nine
National Energy Technology Laboratory
(304) 285-2017, fax: (304) 285-4469, e-mail: ralph.nine@netl.doe.gov

Technology Program Manager: Lee A. Slezak
U.S. Dept. of Energy - Office of the FreedomCAR and Vehicle Technology Program
(202) 586-2335, fax: 586-2476, e-mail: lee.slezak@hq.doe.gov

This report was prepared with the support of the U.S. Department of Energy, under Award No. DE-FC26-04NT42189. However, any opinions, findings, conclusions, or recommendations expressed herein are those of the author(s) and do not necessarily reflect the views of the DOE.

DISCLAIMER

TABLE OF CONTENTS

This report was prepared with the support of the U.S. Department of Energy, under Award No. DE-FC26-04NT42189. However, any opinions, findings, conclusions, or recommendations expressed herein are those of the author(s) and do not necessarily reflect the views of the DOE.

EXECUTIVE SUMMARY

The Advanced Electric Systems and Aerodynamics for Efficiency Improvements in Heavy Duty Trucks program (DE-FC26-04NT42189), commonly referred to as the AES program, focused on areas that will primarily benefit fuel economy and improve heat rejection while driving over the road.

The AES program objectives were to:

- Analyze, design, build, and test a cooling system that provided a minimum of 10 percent greater heat rejection in the same frontal area with no increase in parasitic fan load.
- Realize fuel savings with advanced power management and acceleration assist by utilizing an integrated starter/generator (ISG) and energy storage devices.
- Quantify the effect of aerodynamic drag due to the frontal shape mandated by the area required for the cooling system.

The program effort consisted of modeling and designing components for optimum fuel efficiency, completing fabrication of necessary components, integrating these components into the chassis test bed, completing controls programming, and performance testing the system both on a chassis dynamometer and on the road.

Emission control measures for heavy-duty engines have resulted in increased engine heat loads, thus introducing added parasitic engine cooling loads. Truck electrification, in the form of thermal management, offers technological solutions to mitigate or even neutralize the effects of this trend. Thermal control offers opportunities to avoid increases in cooling system frontal area and forestall reduced fuel economy brought about by additional aerodynamic vehicle drag. This project explored such thermal concepts by installing a 2007 engine that is compliant with current regulations and bears additional heat rejection associated with meeting these regulations. This newer engine replaced the 2002 engine from a previous project that generated less heat rejection.

Advanced power management, utilizing a continuously optimized and controlled power flow between electric components, can offer additional fuel economy benefits to the heavy-duty trucking industry. Control software for power management brings added value to the power distribution and energy storage architecture on board a truck with electric accessories and an ISG.

The research team has built upon a previous truck electrification project, formally, “Parasitic Energy Loss Reduction and Enabling Technologies for Class 7/8 Trucks”, DE-FC04-2000AL6701, where the fundamental concept of electrically-driven accessories replacing belt/gear-driven accessories was demonstrated on a Kenworth T2000 truck chassis. The electrical accessories, shown in Figure 1, were controlled to provide “flow on demand” variable-speed operation and reduced parasitic engine loads for increased fuel economy. These accessories also provided solutions for main engine idle reduction in long haul trucks. The components and systems of the current project have been integrated into the same Kenworth T2000 truck platform.

Figure 1 More Electric Truck

Reducing parasitic engine loading by decoupling accessory loads from the engine and driving them electrically has been a central concept of this project. Belt or gear-driven engine accessories, such as water pump, air conditioning compressor, or air compressor, are necessarily tied to the engine speed dictated by the current vehicle operating conditions. These conventional accessory pumps are sized to provide adequate flow or pressure at low idle or peak torque speeds, resulting in excess flow or pressure at cruising or rated speeds. The excess flow is diverted through a pressure-minimizing device such as a relief valve thereby expending energy to drive unnecessary and inefficient pump operation. This inefficiency causes an increased parasitic load to the engine, which leads to a loss of usable output power and decreased fuel economy.

Controlling variable-speed electric motors to provide only the required flow or pressure of a particular accessory system can yield significant increases in fuel economy for a commercial vehicle. Motor loads at relatively high power levels (1 – 5 kW, or higher) can be efficiently provided current from high-efficiency

This report was prepared with the support of the U.S. Department of Energy, under Award No. DE-FC26-04NT42189. However, any opinions, findings, conclusions, or recommendations expressed herein are those of the author(s) and do not necessarily reflect the views of the DOE.

generators or batteries with system voltages in the range of 250 to 360 volts DC (VDC).

In the previous project, the electric accessories could be powered from one of three sources: an AC voltage source ("shore power"), an on-board diesel generator (auxiliary power unit), or an ISG located in the flywheel housing and driven by the main engine. The electric accessories and power sources, including the ISG, have remained in place for the current upgrade of the research platform vehicle. In this project, more emphasis has been placed on determining the best way to use the ISG to power the vehicle and accessories, thereby yielding additional value from existing hardware.

Investigation of the thermal management system comprised chassis dynamometer testing for both fuel economy and ambient capability. Meanwhile, the concepts of how to most effectively use the ISG and energy storage system were examined during on-road testing. Table 1 summarizes the results of ambient capability testing, showing the gains produced by the AES cooling module. The baseline cooling module proved inadequate for the additional heat rejection requirements of the 2007 engine. The AES cooling module, however, brought ambient capability up to a more conventional 43 °C. Significantly, the AES cooling module required no alterations to the frame or the aerodynamics of the truck chassis.

Table 1 Ambient Capability Test Results

	Baseline	AES	Baseline	AES
Engine Speed (rpm)	1350	1350	1500	1500
Ambient Capability (°C)	40.2	46.4	36.5	42.7

Table 2 highlights the projected impact of the AES components versus the results obtained during vehicle testing. The savings delivered by AES components could be coupled with the improvements of the initial MET project to offer fuel savings on the order of 10 percent. Therefore, some of the same components that accommodate additional heat rejection also offer significant fuel savings.

Table 2 Projected vs. Actual Fuel Economy Improvements

Advanced Electric Systems	Projected Fuel Economy Improvement (%)		Actual Fuel Economy Improvement (%)
	Low	High	
Aerodynamic Drag	0.0	3.0	0.0
Advanced Power Management	1.0	4.0	2.3
Elevated Coolant Temperature	0.5	1.0	0.5
Auxiliary Oil Cooler	0.2	0.5	0.2
High Efficiency Aftercooler	0.2	0.5	1.5
Electric Cooling Fan	0.0	1.0	
Total AES:	1.9	10.0	4.5
More Electric Truck			
MEI Components	1.0	2.0	1.0
Idle Reduction	5.0	7.0	5.0
Total MET:	6.0	9.0	6.0
Total MET & AES:	7.9	19.0	10.5

The transition to broad commercial applications of these technologies in the trucking industry should lead to significant gains in performance, reliability, serviceability, and system design flexibility. The Class 8 truck sector may benefit the most due to their higher average speeds, the large number of vehicles produced yearly, and the high number of miles per year accumulated by each vehicle. Better fuel economy can accompany emissions reduction and could encourage customers to purchase the vehicles as an improved capital investment. These technology enhancements show the potential to be directly beneficial to mobile construction equipment, a variety of commercial and marine engine markets, and powertrains used by a wide variety of U.S. military mobile equipment as well.

ANALYSIS AND DESIGN

Cooling Module

In alignment with the project goal of controlled thermal management for cooling system performance improvements, an electric cooling fan, radiator coolant bypass control valve, and oil cooler were identified as having the potential to increase cooling system heat rejection and efficiency. Simulation analysis showed the AES cooling system with thermal management is capable of 335 kW heat rejection under worst-case ambient condition of 43 °C for both peak torque and rated speed conditions. This includes 227 kW from the water/glycol system and 108 kW from the charge air cooler. Figure 2 is a schematic of the fluid flow through the system.

This report was prepared with the support of the U.S. Department of Energy, under Award No. DE-FC26-04NT42189. However, any opinions, findings, conclusions, or recommendations expressed herein are those of the author(s) and do not necessarily reflect the views of the DOE.

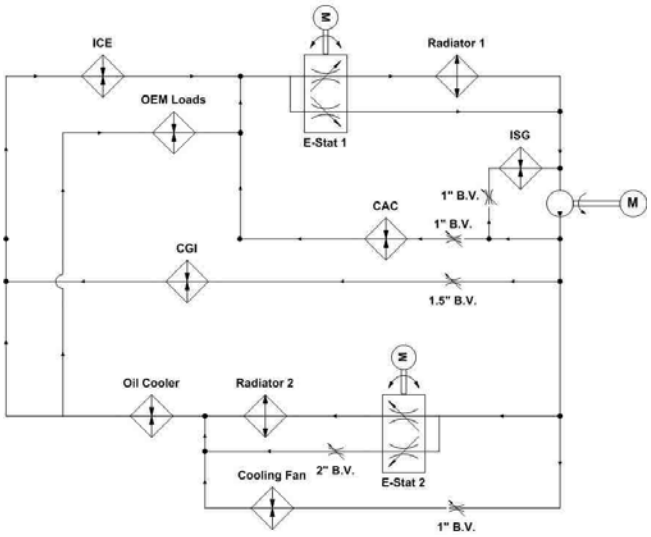

Figure 2 AES Water Cooling Circuit

Electric Cooling Fan

Conventional engine cooling fans on heavy-duty trucks range in size from about 28 inches to 32 inches in diameter and can consume up to 50 kW under conditions of full engine speed and low vehicle speed, especially as engine-to-fan belt pulley speed ratios have increased to about 1.4:1. The fan is belt driven through an on-off clutch on the front of the engine. For a long haul truck, average fan-on time as a percentage of truck operation is about 6 percent with half of that time attributable to air conditioning demands. The cooling fan is typically sized to deliver adequate cooling air flow at a peak torque engine speed of 1200 rpm resulting in excess air delivery at higher engine speeds with a cubic exponential increase in parasitic power draw from the engine. Electrification of the fan allows fan speed to be matched proportionately to cooling system load.

For the electric cooling fan, the space constraints for installation in the current platform were a determining factor in the decision to use a puller-type fan. Hood profile and mounting considerations of truck frame rail ends would have otherwise required a difficult redesign of major structural components. Future designs using an electric pusher fan with the electric motor in front of the heat exchangers have potential to benefit from increased fan efficiency due to the fan blades blowing colder, denser air. Air cooling of the fan motor may also be more feasible with a pusher design, as the motor would be located in cooler air upstream from the heat exchangers.

For the current puller design, fan motor power was specified to 20 kW continuous at 2000 rpm. Thermal challenges in the form of 80 °C air temperatures and 100 °C coolant temperatures combined with space claim constraints to limit fan motor continuous power to about 20 kW. This matches the 20 kW mechanical fan power at 1800 rpm engine speed and 30 mph ram air for a conventional belt-driven fan. With a higher efficiency fan and shroud, the same fan power will give more airflow and yield higher heat rejection.

Switched Reluctance Drives Ltd., a subsidiary of Emerson Electric Co., designed, developed, and tested the prototype electric fan motor shown in Figure 3. The motor uses switched reluctance technology with an 18/12 stator/rotor pole structure and peak continuous power rating of 20 kW at 2000 rpm. Motor operation allows the reversal of the fan, potentially useful to aid hot shutdown of the engine or debris cleanout in an off-highway machine. Motor physical size is approximately 300 mm in diameter by 200 mm in axial length. Electric current commutation is provided by position sensors mounted to the motor front interfacing with slotted tabs on the fan hub. Fan motor/drive efficiency of over 90 percent was demonstrated in dynamometer testing over most of its operating speed and power range.

Figure 3 20kW Cooling Fan Motor

Primary cooling of the motor stator windings is accomplished with engine coolant, while an aft-to-fore air-cooling stream through openings in the motor endplates provides secondary rotor/stator cooling. Radial vanes on the fan hub provide a negative pressure zone at the motor front, enabling cooling airflow through the rotor.

The fan hub, Figure 4, was designed to wrap around the motor and provide mounting for the base of nine individually molded blades. This wraparound design allowed the fan blade leading edge to be located 100 mm from the radiator core, improving efficiency of the airfoil shaped blades and permitting space for the inlet radius of a type II shroud. Centrally locating the fan relative to the radiator core and a tight tip to shroud clearance allowed a fan diameter of 864 mm in contrast to the 812 mm diameter of the baseline system of the MET.

This report was prepared with the support of the U.S. Department of Energy, under Award No. DE-FC26-04NT42189. However, any opinions, findings, conclusions, or recommendations expressed herein are those of the author(s) and do not necessarily reflect the views of the DOE.

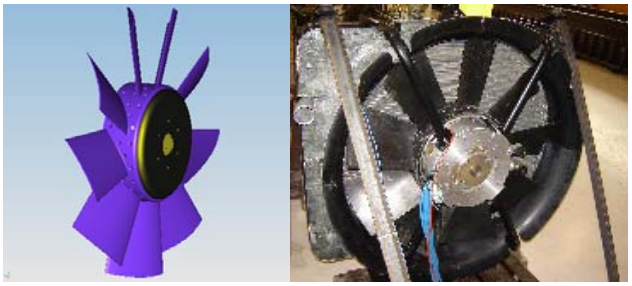

Figure 4 Fan Hub and Blade Design

The AES cooling module consists of the electric fan mounted to the aft side of the radiator frame and the auxiliary oil cooler and charge air cooler mounted to the front of the radiator frame. The electric cooling fan and motor were designed to integrate with the cooling module through cross frame tubing supports mounted to each corner of the radiator frame. Mounting to the radiator frame allowed close tip-to-shroud tolerance (8mm) since there was no need to account for engine movement on flexible mounts. Mounting the cooling fan and motor to the radiator frame also permitted a completely modular cooling package design for easy assembly and service. This cooling module can be assembled as a unit and then mounted as one piece to the truck frame.

To verify operation of the fan motor in a controlled environment, the cooling module was mounted to a bedplate and operated in a test cell. Operation of the fan mounted to the radiator frame was validated to 1500 rpm and 15 kW of electrical input power. System control and communications with the fan drive were verified. The fan was tested for excessive vibrations at natural frequencies that could cause damage to the fan or frame. The design and mounting were found to be robust and ready for integration to the vehicle with no excessive vibrations throughout the speed range of the fan.

Computational fluid dynamics (CFD) analysis for T2000 underhood cooling airflow was performed for both the baseline conventional cooling components and the new AES components. Figure 5 shows velocity vectors in a horizontal plane view of the engine compartment – one of many CFD snapshots captured.

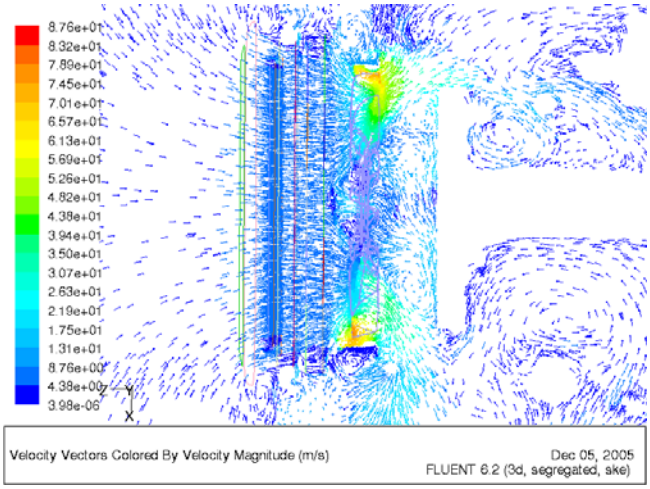

Figure 5 Horizontal Plane Velocity Vectors of Baseline Configuration

Results of the underhood CFD cooling analysis using AES components (see Table 3) showed an overall 14-33 percent efficiency gain (fan power (kW) per fan flow (kg/s)) with the AES fan and shroud design. The range stemmed from analysis at different design points with variable fan and vehicle speeds. Most significant was the 33 percent efficiency gain at the worst case cooling point of full fan speed (2000 rpm) and low ram air speed (30 mph) where the fan delivered 10.3 kg/s airflow with a mechanical input power of 28.9 kW (power to flow ratio 2.81). This compared favorably to analysis of the vehicle baseline belt-driven fan (see Table 4) delivering 12.0 kg/s at 2520 rpm with an input power of 50.0 kW (power to flow ratio 4.17).

Table 3 AES Cooling Components

	Fan speed (rpm)	Ram air (mph)	Grill flow (kg/s)	Fan flow (kg/s)	Fan power (kW)	Fan power /Fan flow (kJ/kg)
Baseline	1500	0	4.8	7.2	12.1	1.68
Iteration 1	1500	30	6.6	7.6	12.2	1.60
Iteration 2	1500	60	9.9	8.6	12.5	1.46
Iteration 3	2000	30	8.2	10.3	28.9	2.80

Table 4 Baseline Conventional Cooling Components

	Fan speed (rpm)	Ram air (mph)	Grill flow (kg/s)	Fan flow (kg/s)	Fan power (kW)	Fan power /Fan flow (kJ/kg)
Baseline	1680	0	4.5	6.7	13.0	1.94
Iteration 1	1680	30	6.7	7.8	14.6	1.87
Iteration 2	1680	60	10.3	9.4	17.8	1.90
Iteration 3	2520	30	9.1	12.0	50.0	4.17

Laboratory airflow tests were conducted with the newly fabricated fan blades, hub, and type II venturi shroud. These components were mounted in the fan laboratory air testing plenum, where variable

This report was prepared with the support of the U.S. Department of Energy, under Award No. DE-FC26-04NT42189. However, any opinions, findings, conclusions, or recommendations expressed herein are those of the author(s) and do not necessarily reflect the views of the DOE.

restriction was used to develop static pressure. The fan was driven by an electric motor and a transducer was used to measure torque.

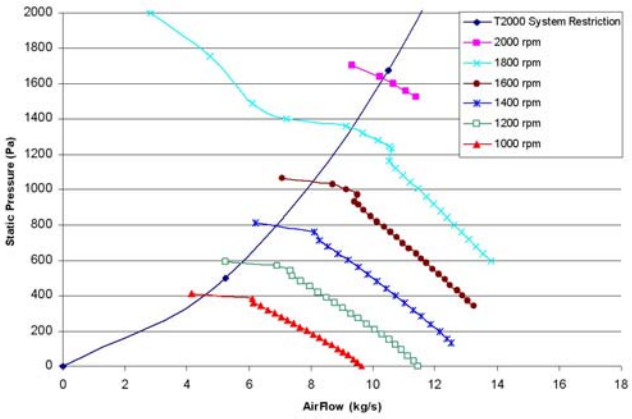

Figure 6 AES Fan Pressure versus Airflow

Figure 6 shows the test pressure curves versus airflow for various fan speeds, while Figure 7 shows the mechanical power measured to produce the pressure and flow of Figure 6.

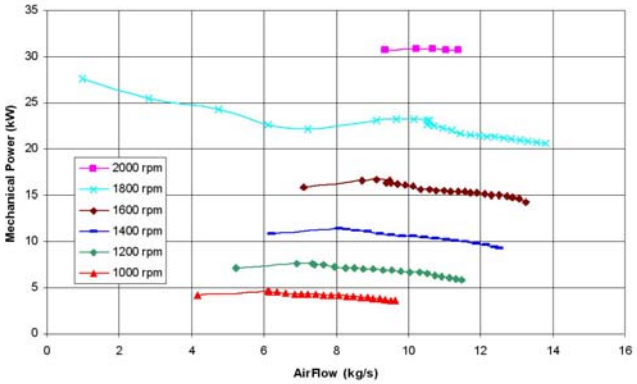

Figure 7 AES Fan Mechanical Power versus Airflow

Using fan curves obtained for the 812 mm T2000 baseline fan and the T2000 restriction curve from Figure 6, flow and power curves versus speed were developed for the baseline fan (not shown). Figure 6 and Figure 7 were used to construct similar curves of flow and power versus speed for the AES fan design. Figure 8 shows a comparison plot of the baseline fan versus the AES fan. The results showed a 7 percent increase in airflow for the same mechanical input power, 23.1 kW. It was also noted that the AES fan, at a larger (864 mm) diameter than the baseline fan, is a more aggressive design, and will produce equal airflow at lower rotational speeds. To produce similar airflow, 9.3 kg/s, the AES fan required 23.1 kW, while the baseline fan needed 28 kW of mechanical input power, translating to a 17.5 percent increase in efficiency with the new AES design versus the baseline fan. This efficiency increase is important, since the energy conversion of mechanical to electrical power from the ISG and back to mechanical power in the fan motor increased the overall parasitic power load to the engine. Using the 90 percent efficiency of the ISG and fan motor obtained during testing resulted in 28.5 kW of engine power required to drive the electric fan at full power. This compared favorably to the 28 kW mechanical input power at 2100 rpm, where additional engine power (2-5 percent) would be lost through the belts driving the fan.

The 23 kW mechanical input power on the plot of Figure 8 is significant, as this is about the maximum that the fan motor is capable of producing at 1800 rpm. Given the system restriction curve shown in Figure 6, the electric fan would be power limited to about 1800 rpm, even though it was characterized and tested to 2500 rpm (at constant 23 kW power over the 1800 to 2500 rpm range).

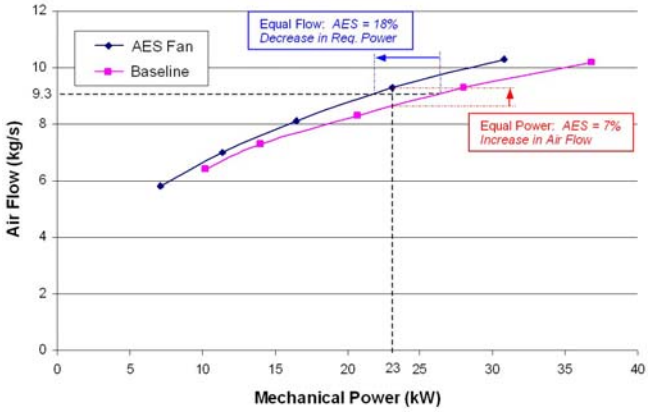

Figure 8 Comparison of Baseline and AES Fan Power and Flow

The above analysis encompasses worst-case operational conditions for the cooling fan at maximum heat rejection load. The real advantage of the electric fan is its variable speed operation, so that at normal operating conditions when less heat rejection may be required from the cooling system, the fan motor is controlled to a speed proportional to the heat rejection load. Since the power draw of a fan is proportional to the cube of speed, the electric fan significantly reduces the parasitic engine load for a majority of the operational conditions compared to an on/off clutched, belt-driven fan.

Table 5 shows a comparison of the energy consumed during an hour of operation for both a belt-driven fan operating at a 5 percent on-duty cycle at 1980 rpm and an electric fan operating at 100 percent on-duty cycle at 500 rpm. The electric fan moves nearly 3.5

This report was prepared with the support of the U.S. Department of Energy, under Award No. DE-FC26-04NT42189. However, any opinions, findings, conclusions, or recommendations expressed herein are those of the author(s) and do not necessarily reflect the views of the DOE.

times the air mass while using less than half the energy. The constant speed electric fan would also result in a more consistent coolant temperature. This scenario of lower heat rejection requirements may occur during highway cruising or lower speed urban operation of a Class 8 truck.

Table 5 Comparison of Fan Drive Energy

Fan Drive	Duty Cycle (%)	Power (kW)	Energy Used over 1 Hr (kWh)	Airflow (kg/s)	Air Mass Moved over 1 Hr (kg)
Belt-Driven Fan	5	28	1.40	9.3	1674
Electric Fan	100	0.62	0.62	1.6	5760

System controller and fan motor drive communications occur over a controller area network (CAN) using SAE J1939 specifications and proprietary network identifiers (IDs). Supervisory control algorithms for speed control of the cooling fan motor were developed to provide the temperature differential across both radiator and engine to within an 8 °C range. The fan only operates when the bypass valve is routing all coolant to the radiator. This ensures the diverter valve primarily controls coolant temperature, as this is the control actuation with the least energy cost. The fan then operates in variable speed mode to control the temperature differential across the radiator.

Radiator Coolant Bypass Control Valve

An electrically-actuated valve was supplied by Engineered Machined Products, Inc. to control the coolant flow between the radiator and radiator bypass loop of the coolant circuit. Replacement of a conventional wax-type thermostat allowed for variable set point engine coolant temperatures. During periods of light to moderate engine load, the reference temperature can be increased, thus allowing less heat absorption by the coolant from the engine and permitting higher exhaust temperatures for better passive regeneration of the diesel particulate filter (DPF). The increased exhaust energy can also be used to power more boost from the turbocharger. Higher coolant temperature can also result in elevated cylinder wall temperature, increasing combustion efficiency. As engine load increases, the temperature set point can be decreased to provide adequate cooling of exhaust ports and other areas of high heat concentration. The device also offers opportunities to improve cooling system filling via its electronically actuated full range of motion.

Figure 9 shows the valve installation in the research platform integrated with the C15 engine. The control valve consists of a linearly-actuated flow diverter contained in a cylindrical nylon and aluminum housing driven by a stepper motor. A small drive electronics box with CAN communication and current drivers for the valve motor/actuator runs from the vehicle 12 V power. The 2.4-inch valve with 1-inch bypass provides 100 gallons per minute (gpm) flow with a 1-psi pressure drop, 300 gpm with a 5-psi pressure drop, and goes from closed to full open in 16 seconds. As with the fan, communication between the supervisory controller and the valve electronics is established via CAN using SAE J1939 specifications and proprietary network IDs.

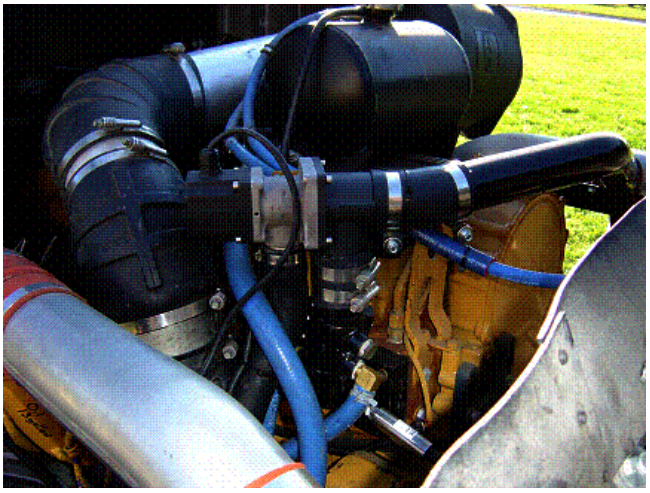

Figure 9 Radiator Coolant Bypass Control Valve Installation

The design requirements for the valve included:

- Reference temperature easily adjusted
- Engine coolant temperature controlled to +/- 5 °C around the reference temperature
- System heat rejection maximized solely through valve actuation, minimizing the water pump and fan usage
- Small unnecessary movement of the valve (valve hunting) minimized
- Warm up time of the engine decreased
- ΔT of the coolant temperature across the block minimized to a maximum of 8 °C

A variety of controls strategies were tested against both the virtual truck/engine system and on the actual T2000 truck itself in order to devise a responsive system to provide optimal cooling. Proportional and proportional plus integral feedback control systems based on engine coolant temperature experienced coolant transport delays and temperature sensor data transmission delays. With these delays, it was difficult to achieve reasonable system response times without having high control gain levels that made the system unstable. Neural network algorithms for this

This report was prepared with the support of the U.S. Department of Energy, under Award No. DE-FC26-04NT42189. However, any opinions, findings, conclusions, or recommendations expressed herein are those of the author(s) and do not necessarily reflect the views of the DOE.

application were created based on engine torque levels as a solution to help give the control system more of a predictive response.

Auxiliary Oil Cooler

The elevated engine coolant temperature made possible by the radiator coolant bypass control valve necessarily results in increased radiator outlet temperature, or bottom tank temperature, given that a temperature differential of 8 °C or less must be maintained across the engine. Since it is the coolant from the radiator outlet that is used to absorb heat in the oil cooler (oil to coolant heat exchanger), an increase in the bottom tank temperature may result in an inadequate temperature gradient across the oil cooler to effectively cool the engine oil. To mitigate this effect, the concept shown in Figure 10 was implemented to provide supplementary cooling of the coolant entering the oil cooler. The liquid-to-air heat exchanger is integrated into the vehicle cooling module with the radiator and charge air cooler.

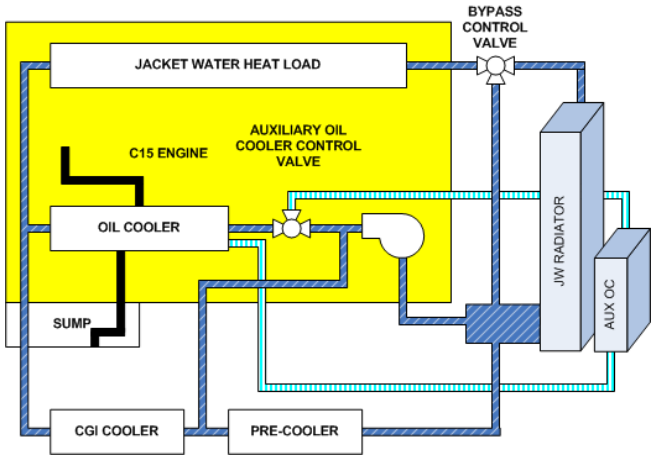

Figure 10 Oil Cooling System

The auxiliary oil cooler control valve shown in Figure 10 provides control over the temperature of the coolant entering the oil cooler. In principle, by using the proportional flow control valve, the engine oil temperature, and ultimately the temperature dependent viscosity of the oil, can effectively be controlled. In this way, during times of light to moderate engine loading and especially at low ambient temperatures, the oil temperature can be increased to reduce oil viscosity and parasitic friction. For periods of high engine loading, the oil temperature can be decreased to provide adequate oil pressure for journal bearing flotation and critical cooling of engine components by the engine oil.

High Temperature (Hi-Temp) Aftercooler

The original intent of the project's high temperature aftercooler (charge air cooler) design was to have copper fins brazed to brass tubes, as the copper and brass material possessed high strength over the operating temperature, and high thermal conductance. The development of the copper/brass aftercooler was abandoned due to condensation of acidic exhaust components in the charge air and the relatively low resistance of brass and copper to corrosion caused by the acidic condensate. The prime path for the aftercooler design called for corrosion resistant stainless steel.

The aftercooler was designed according to the following constraints:

- NO_x emissions reduction strategies, in the form of recirculation of clean, hot exhaust gas, and associated increase in total charge air mass flow, have resulted in higher charge air temperature and increased heat removal necessary by the aftercooler.
- Current aluminum aftercooler does not have the material properties to withstand higher temperatures, necessitating an air to jacket water pre-cooler.
    a. Pre-cooler adds restriction and results in increased pumping losses to both air and coolant.
    b. Stainless steel material properties of aftercooler allow it to withstand higher temperatures.
- More efficient aftercooler design can further reduce parasitic pumping losses and increase heat rejection per unit area.
- Increased heat rejection per unit area can result in reduced frontal area of aftercooler, reducing overall vehicle drag.

Conventional design of tube-fin extended surfaces consists of flat tubes with internal turbulators (offset strip fins, v-shape) for charge air and external fins for cooling air (wave type fins). The new hi-temp aftercooler employs a primary surface tube with external fins - narrower flat tubes with internal dimples/ribs (no fins) as a primary heat transfer surface for charge air and with conventional external fins for cooling air. A highly optimized turbulator design gently rolls charge air, avoiding stratified temperature differential of laminar airflow, yet preventing highly turbulent flow that would cause an excessive pressure drop across the aftercooler. A significant advantage of the design was a reduction in charge air tube width by as much as 50 percent, for increased surface area/volume ratio, providing increased heat transfer. This results in equal rate of

This report was prepared with the support of the U.S. Department of Energy, under Award No. DE-FC26-04NT42189. However, any opinions, findings, conclusions, or recommendations expressed herein are those of the author(s) and do not necessarily reflect the views of the DOE.

heat transfer from charge air (compared with conventional charge air cooler on unit area basis), with less charge air pressure loss, increased heat transfer to cooling air, and decreased cooling air pressure loss. The design also allowed for higher strength tubes to withstand higher temperatures and pressures. Overall, the high-temperature aftercooler permitted elimination of the charge air pre-cooler, lower parasitic charge air pressure loss, and increased cooling airflow.

Aerodynamic Drag Study

Argonne National Laboratory (ANL) also conducted research related to the cooling package. ANL studied the effects of small changes in radiator configurations on the aerodynamic performance of an aerodynamic tractor-trailer truck. These effects were quantified through a series of parametric engineering design studies using CFD simulations. A nominal geometry based on the Generic Conventional Model (GCM) was developed and the modified geometries were defined by altering the dimensions of the GCM using commercial CAD software. This approach has been developed as part of Argonne's contributions to the U.S. Department of Energy's Heavy Vehicle Aerodynamic Working Group.

This study considered four different configurations for the radiator with different conditions to test for each configuration. The analysis included changes to grill/radiator height, grill/radiator width, grill/radiator surface area (maintaining the aspect ratio for the surface), and grill/radiator tilt with respect to the vertical axis of the vehicle. The primary radius of curvature between the hood panels and between the top of the hood and the grill was maintained in all cases. In all cases, no significant change was found in the total amount of drag force on the vehicle but there were changes to the distribution of that force across the grill/radiator area.

Based on the study results, the ANL team concluded that small changes in radiator size, either reduction or expansion, did not affect the fuel economy in any significant way if the vehicle was reasonably aerodynamic already. Small changes in radiator tilt also had a limited effect for reasonably aerodynamic vehicles. The ANL team goes on to suggest that these small changes might have more fuel economy effect for tractor-trailer vehicles that are not already optimized for aerodynamics.

Advanced Power Management

Management of the ISG and energy storage system (ESS) wields significant influence over the improvements wrought by an electrified architecture. The project explored advanced power management of electrified accessories and hybrid operation with electric energy storage. Proper use of the ISG and ESS during acceleration and deceleration offer the potential to increase fuel economy significantly depending on the drive cycle the vehicle undergoes.

Initially, a combined Dynasty plant model and Simulink® control model of the MEI truck was used in a comparative evaluation of a possible power management control. The vehicle powertrain and accessory loads were modeled in Dynasty. Mechanical and electric accessories could easily be applied or removed to analyze the performance of both. Control algorithms were developed in Simulink® to facilitate porting from simulations to the actual vehicle controller. In an initial acceleration assist scheme, the ISG acted as a motor when the engine was under heavy load (greater than 80 percent of maximum torque). The ISG and other accessories ran off the high-voltage battery during this time. When the engine load decreased, or if the battery charge fell below a lower limit (70 percent of maximum charge), the ISG switched back to generator mode and recharged the battery.

The following table compares the fuel usage results of the simulation for the MEI truck traveling on a sinusoidal (hilly) road profile for a distance of 100 km. The elevation frequency is the distance between peaks along the route. Table 6 suggests that the fuel savings are highly dependent on the road profile, with this particular strategy even demonstrating a decrease in fuel economy for some road profiles. Nevertheless, these results are unique to the control strategy described above, and later efforts continued to examine methods to better match the control strategy to various road profiles.

Table 6 Simulated Fuel Usage with a Motor/Generator Power-Management Control

Maximum Grade (%)	Elevation Frequency (km)	Fuel Usage w/o Pwr Mgmt (liters)	Fuel Usage w/ Pwr Mgmt (liters)	Difference (%)
4	5	56.3	55.0	-2.31
2	5	41.5	39.9	-3.86
4	10	52.7	52.0	-1.33
2	10	39.2	39.6	+1.02

In addition, modeling and simulation with the objective of using the ISG for launch assist of the truck was undertaken. The truck's motion in terms of velocity, acceleration, and jerk at start-up in 2nd, 4th, and 6th gears was evaluated. The analysis suggested that with the engine at warm temperature (coolant above 70 °C), the ISG would have the torque capability to launch the truck, even fully loaded, on level ground, with clutch engaged, while concurrently bringing the engine up to starting speed. This capability is a key

This report was prepared with the support of the U.S. Department of Energy, under Award No. DE-FC26-04NT42189. However, any opinions, findings, conclusions, or recommendations expressed herein are those of the author(s) and do not necessarily reflect the views of the DOE.

enabler of start/stop operation and further increases the overall value of an ISG to the end customer, in terms of increased functionality and overall fuel savings opportunities.

In response to the desire for launch assist, an algorithm to simultaneously launch and start the engine during periods of frequent stop-and-go traffic was refined and demonstrated on the truck. This new functionality permits idle stop, or shutdown of the engine, saving fuel and reducing emissions. In addition to restarting the engine, the ISG also provides initial propulsion of the truck as soon as the driver pushes the accelerator pedal. Acceleration assist and cruise assist then proved to be natural extensions of the launch assist algorithms. Acceleration assist provides power when increased vehicle speed is desired. Cruise-assist capability was next added to the power management algorithm. Cruise assist switches the ISG from generating to motoring to help maintain a constant travel speed during times of increased engine load, such as when going uphill. As noted in Table 6, simulation analysis indicated that fuel savings of 1-4 percent were possible with a cruise-assist control, depending on the spacing and steepness of the hills

To make use of the assist algorithms, motoring capability was added to the internal algorithms of ISG. Sensorless control algorithms for the ISG were developed for motoring operation over the 0 to 2400 rpm range by Emerson's Switched Reluctance Drives (SRD) division. Peak torque of 1200 Nm was achieved from 0 to 160 rpm and constant power of approximately 25 kW was achieved from 500 to 2400 rpm with 84 percent to 90 percent efficiency.

Figure 11 shows a plot of an engine off stop/start operation with the ISG. With the sizeable peak torque capability of the ISG, simultaneous engine starting and vehicle launch from a vehicle stop is possible, even with a fully loaded trailer and gross vehicle weight (GVW) of 80,000 lbs. Idle stop and launch assist for heavy-duty applications have the potential to increase and smooth vehicle acceleration and to reduce clutch wear. Engine load transients may also be reduced during launch assist, providing possible reduction in emissions.

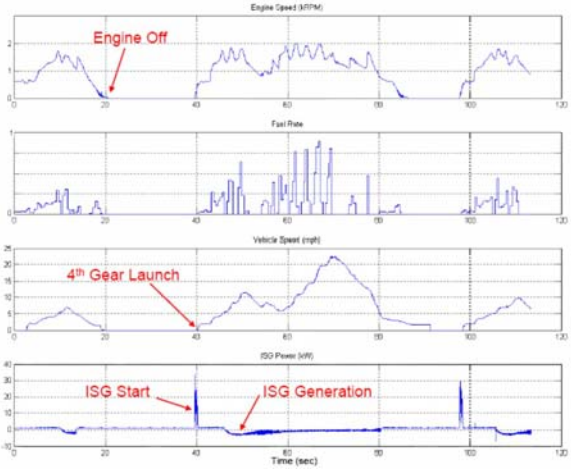

Figure 11 ISG Plots showing Engine Stop/Start Assist

The vehicle operations and assist modes described previously clearly rely on energy storage to add mechanical power to the driveline. An electrical energy storage system using nickel-metal hydride batteries was specified for typical heavy-duty over-the-road drive cycles. Key factors of life cycle versus depth of discharge, peak power delivery and absorption, and charge/discharge efficiency were used for system sizing. The 4.8 kWh system was initially specified to allow 100 seconds of acceleration or deceleration with a 20 percent depth of discharge. Subsequent testing has revealed that the battery pack could be downsized for many applications.

Once again the Dynasty and Simulink® models of the truck were used for controls development before the final algorithms were placed in the truck's supervisory controller. This development produced algorithms for regenerative braking, cruise overspeed regeneration, and charge maintenance. Also, initial tuning of the closed-loop generator control was implemented in simulation. The regenerative braking algorithm becomes active when the vehicle's brake pedal is depressed provided the battery state of charge (SOC) does not exceed a maximum value of 70 percent and the vehicle speed is above a minimum threshold. The cruise overspeed regeneration algorithm serves as the core algorithm of on-highway, high-speed operation. It uses the cruise control set speed and the actual vehicle speed to determine the downhill portion of the drive cycle. During the downhill portion, the generator charges the battery as long as the battery's SOC does not exceed a maximum value. The maintain charge algorithms use closed-loop control of the generator to maintain the minimum SOC of the battery if conditions allowed for the SOC to drop this low. This strategy prohibits fuel usage for battery charging above the minimum SOC. The key to this

This report was prepared with the support of the U.S. Department of Energy, under Award No. DE-FC26-04NT42189. However, any opinions, findings, conclusions, or recommendations expressed herein are those of the author(s) and do not necessarily reflect the views of the DOE.

strategy is to use regenerative energy rather than crankshaft energy to maintain energy reserves. The cruise assist algorithm activates when the SOC is between 55 percent and 70 percent and engine load is in a part-load range. Shutting off the motor at 55 percent SOC was meant to allow for accessories to drain the SOC from 55 percent down to 50 percent before the generator needed to turn on again. Only operating cruise assist at part-load allows the motor to use excessive battery energy when power is needed in the drivetrain without enhancing performance during periods of peak load. Assisting at part-load reduces the engine fuel rate whereas assisting at peak load does not reduce the engine fuel rate. While peak load supplementation might prove beneficial at times, the strategy employed focused on overall fuel economy returns.

Engine Upgrade

A 2007 emissions-compliant, pre-production Caterpillar® C15 engine was procured and installed in the T2000 vehicle test platform. This C15 ACERT™ engine, rated at 550 hp and 1850 ft-lb of torque, includes a DPF and a Caterpillar Regeneration System (CRS). The decision to upgrade to the 2007 engine was made in order to demonstrate the electric accessory and power management technology on an engine with 2007 representative heat loads and heat load splits.

TESTING AND RESULTS

Chassis Dynamometer Testing

Chassis dynamometer testing was performed during May and June 2007 in laboratory facilities at Caterpillar Inc. The objectives of the chassis dynamometer testing were to:

- Verify the fuel consumption of the Kenworth T2000 test truck in a baseline test chassis configuration (without use of cooling system electrification).
- Evaluate fuel economy improvements resulting from truck electrification and running at elevated top tank temperatures as compared to the baseline test chassis configuration.
- Evaluate and document vehicle ambient capability for full AES configuration and baseline test chassis configuration at 1500 rpm and 1350 rpm.

The baseline test chassis was the Kenworth T2000 truck equipped with a pre-production 2007 Caterpillar 550 hp C15 engine and the initial 2002 cooling system from the More Electric Truck project. This configuration included a mechanical water pump, mechanical fan, and mechanical thermostat. The AES test chassis configuration comprised the aforementioned modifications including an electric water pump, electric cooling fan, electric thermostat valve, and a newer cooling module. In both the baseline and AES tests, the ISG was controlled to provide zero battery current in order remove variation of results due to battery charging or discharging.

The tests included analyzing the baseline test chassis configuration and the AES fully electrified configuration for both fuel economy and ambient capability. The baseline test chassis configuration was tested for fuel rate and those numbers were compared to manufacturer specifications. The baseline test chassis configuration fuel consumption was within 2 percent of the nominal values across the lug curve provided by the engine manufacturer. This initial fuel rate test verified full load capability of the engine so that 25 and 50 percent of full load could be determined and used for fuel economy tests.

Chassis dynamometer testing determined that the top tank ambient capability for the baseline test chassis configuration was 36.3 °C. With the baseline cooling module designed for the heat loads of a 2002 engine, the system might be expected to prove inadequate for a 2007 compliant engine. Analysis suggests that the 2007 engine should produce approximately 50 percent more heat rejection than a 2002 engine. Of significance then, is the ability of the fully integrated AES configuration to raise top tank ambient capability to a more conventional 42.7 °C. Therefore, the implementation of the AES cooling module provides appropriate heat rejection for current engines without structural or aerodynamic modifications to the truck chassis.

Additionally, the full electric accessories configuration produced a 2.7 percent maximum fuel efficiency improvement. This improvement is realized not only through increased efficiency, but also through additional control opportunities. The electric accessories, for instance, also offer the ability to more tightly control top tank temperature as a result of variable speed operation of the water pump and fan, and variable positioning of the electric thermostat. Tightly controlled engine top tank temperature improves heat rejection by reducing the temperature cycling that a conventional clutched fan induces. Smaller oscillations about the temperature setpoint yield a larger average temperature difference between the ambient air and the coolant over the course of operation. As such, test runs were performed at a top tank temperature of 110 °C. Figure 12 shows a comparison of the chassis dynamometer fuel

This report was prepared with the support of the U.S. Department of Energy, under Award No. DE-FC26-04NT42189. However, any opinions, findings, conclusions, or recommendations expressed herein are those of the author(s) and do not necessarily reflect the views of the DOE.

economy results for various configurations compared to the baseline test chassis configuration.

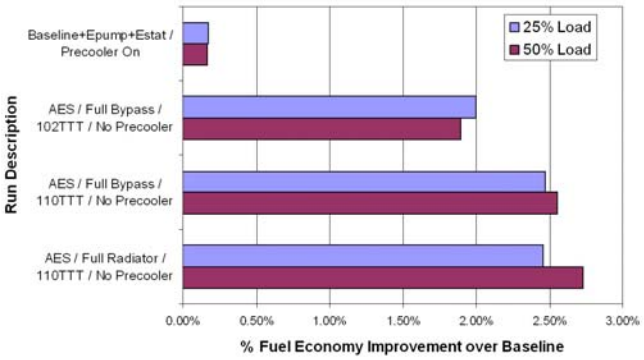

Figure 12 Chassis Dynamometer Results for AES Testing at 1350 rpm and 50 Percent Load

The chart shows fuel economy improvements relative the baseline configuration. The uppermost data point, "Baseline+Epump+Estat Precooler On", portrays the improvement brought by electrifying the water pump and thermostat. Gains here could be attributed to more efficient operation of the water pump and more consistent operating temperatures resulting from electric valve operation. The second data point, "AES/Full Bypass/102 TTT/No Precooler" employs the complete AES cooling module operating with a top tank setpoint of 102 °C. The precooler has been physically removed from the system. The additional heat rejection of the AES module facilitates precooler removal and reduces restrictions in both the air and the coolant circuit. These improvements reduce fan demand and dramatically increase system efficiency as seen previously in Table 5. "Full Bypass" in this context refers to bypassing the auxiliary oil cooler. At approximately 1.5 percent, this step in the transformation clearly yields the largest fuel economy improvement in addition to paving the way for the increased ambient capability. The change to 110 °C for the top tank setpoint comprises the change for the third test markers. Small fuel economy improvements were expected here as a result of combustion efficiency and oil viscosity effects. Finally, the fourth data set diverts coolant through the auxiliary oil cooler. As mentioned, the auxiliary cooler offers additional cooling in the face of the elevated top tank temperature. This gain is small in comparison and the performance is sensitive to sizing and flow rates. Chassis dynamometer performance suggests that further optimization may reveal different flow rates, line/cooler sizes, and/or potentially some schemes that do not require the additional circuit.

The increase in fuel economy clearly demonstrates the enhanced capability and performance improvements of the AES configuration. The bulk of the improvement materialized from the AES cooling module including the electric cooling fan. Improved heat rejection reduces the need for cooling fan power, which is a very effective way to improve fuel economy. Importantly, the improved heat rejection did not require a larger area for the grill opening. Furthermore, the independent operation of the cooling fan allows for steady power consumption from the fan. As previously shown in Table 5, this greatly reduces power consumption with the added benefit of removing the transient loads that a conventional fan would place on the engine.

Road Testing

Road testing was completed in August 2007. The objective of the road test was to conduct fuel economy testing within requirements set forth in both SAE J1321 test procedure type II and "The Fleet Manager's Guide to Fuel Economy" in order to discover the best controls scenario(s) to optimize fuel economy and quantify the percent improvement in fuel consumption.

Testing took place on an interstate route in central Iowa. The test route featured two laps of a 58-mile (one way) route for a total of 232 miles. A test run took just under 4 hours. Each driver remained paired with the same truck and speed was maintained at 65 mph using cruise control to reduce variability. Air conditioning was turned off for each run.

Fuel volume was measured using the procedures outlined in SAEJ1321. A thermometer and hydrometer were used to measure the temperature of the fuel and the fuel specific gravity. A correction factor was applied to the fuel volume based on those measurements.

The road test consisted of testing the AES test truck under three different control modes: baseline (maintaining battery charge), using regenerative braking with no propulsion assist, and using regenerative braking and assisting propulsion during medium-load conditions when battery SOC was sufficient. The test and control trucks ran through a minimum of three runs for each control scenario. In order for the run sets to be considered successful, the test to control (T/C) ratio of each run needed to be within 2 percent of the other runs in that set. Run data that was not within that 2 percent band was disregarded and the run was repeated.

Results shown in Figure 13 illustrate a 2.3 percent improvement in fuel economy when using regenerative braking and a 0.8 percent improvement in fuel economy when using both regenerative braking and the ISG propulsion assist.

This report was prepared with the support of the U.S. Department of Energy, under Award No. DE-FC26-04NT42189. However, any opinions, findings, conclusions, or recommendations expressed herein are those of the author(s) and do not necessarily reflect the views of the DOE.

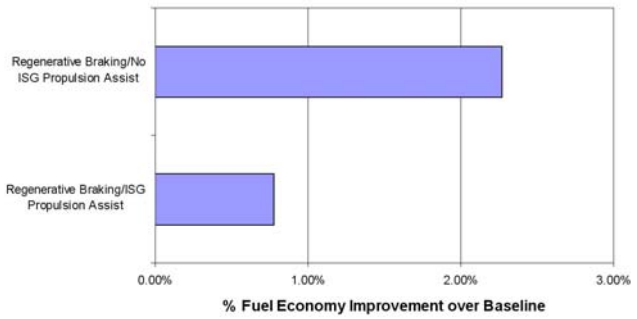

Figure 13 Road Testing Results for AES Testing

The reduction in fuel economy improvement when using additional assistance for the propulsion of the vehicle may, at first, seem counterintuitive. Nevertheless, a few plausible explanations may be found in the fuel consumption characteristics of the engine as well as the nature of vehicle momentum and the impact of the drive cycle on power management logic and fuel savings. In many instances, the addition of ISG power to the driveline reduces the load on the engine. For the same road speed, in the same gear, this reduced engine load can result in decreased efficiency. This phenomenon can be observed in a plot of brake specific fuel consumption (BSFC). BSFC measures the mass of fuel used per unit of mechanical energy out of the engine. Using the ISG assist reduces the engine power operating point by about ~26kW (~35 hp), raising the engine's BSFC, thereby lowering engine fuel efficiency. Figure 14 illustrates the reduction in engine fuel efficiency in a graph of the engine speed versus power output for the engine during this test run.

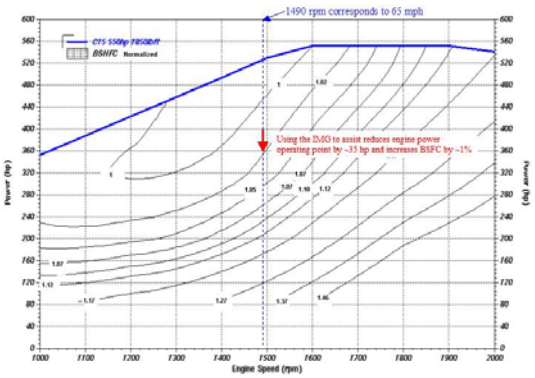

Figure 14 BSFC Map Showing the Impact of ISG Assist

While BSFC considerations may have some impact on fuel consumption, an additional, more significant consideration is the interdependence of the control strategy, cruise control, and the terrain. The testing was conducted with the cruise control set to 65 mph on rolling terrain. Typically, cruise control functions in a "soft" fashion, allowing the vehicle to exceed the setpoint during downhill coasting. The regenerative braking/propulsion assist algorithms may function a bit more aggressively than cruise control during downhill runs to satisfy SOC conditions for the energy storage system. The assist algorithms use the stored energy much more rapidly, thus the system uses the downhill portions to restore the charge. In these cases, the truck may not accrue as much momentum because of the increased duration of regeneration. The reduced momentum therefore might necessitate additional load to traverse the next uphill slope, resulting in additional fuel consumption. This situation will occur if the potential energy the truck can capture during downhill sections of road is more efficiently stored as kinetic energy in the form of momentum rather than storing potential energy in the battery packs. Figure 15 shows the increased time of regeneration and the subsequent loss of vehicle speed in the assist and regenerate configuration.

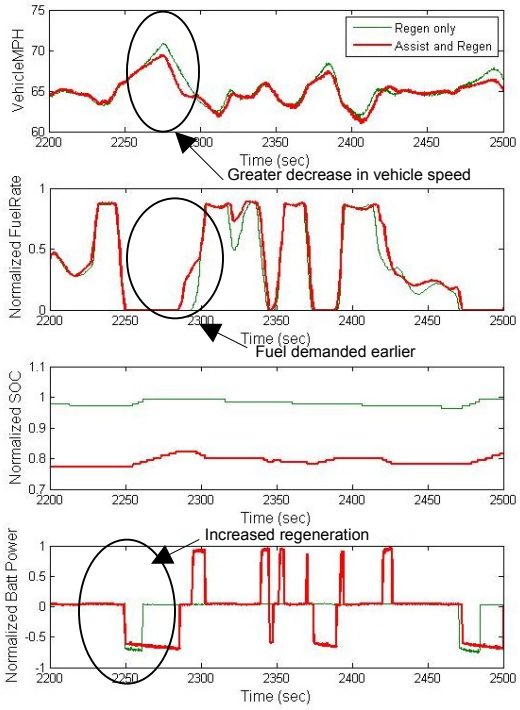

Figure 15 Control Strategy Impact in Hilly Terrain

The plot above shows the vehicle speed along with normalized fuel rate, SOC, and battery power over the same section of road for both the regenerate-only and assist configurations. This plot portrays an example of increased regeneration on the downhill slope reducing the momentum available for the following hill ascent. The reduced momentum causes the vehicle to drop below the set speed earlier, which leads to a net

This report was prepared with the support of the U.S. Department of Energy, under Award No. DE-FC26-04NT42189. However, any opinions, findings, conclusions, or recommendations expressed herein are those of the author(s) and do not necessarily reflect the views of the DOE.

increase in fuel consumption, as fuel is demanded earlier to compensate for the loss in speed.

Figure 16, on the other hand, highlights the SOC for both the regenerate-only and assist configurations over the course of an entire test run. The SOC starts at the same level for both configurations, but it can be seen that in the regenerate-only configuration, the SOC will increase and maintain a level close to the maximum, due to the relatively low accessory load on the truck. The energy used in powering the accessories is easily recaptured through short periods of regeneration on a downhill grade. In the assist configuration, however, the SOC increases a small amount and maintains a level only slightly above the minimum due to the increased energy used to assist. In both configurations the complete depth of discharge is not utilized suggesting that additional optimization of the strategies would benefit the overall consumption.

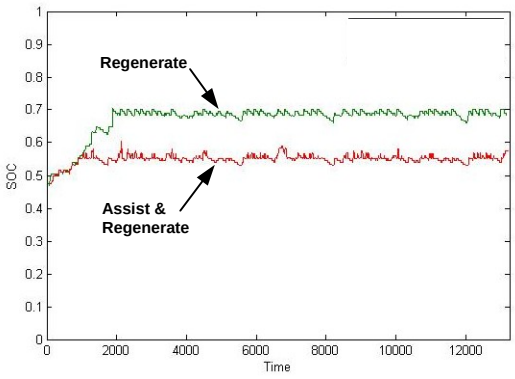

Figure 16 SOC Data for One Test Run

Due to the known dependence of drive cycle on the fuel consumption results, the road profile was scrutinized in additional detail. Figure 17 shows the profile of the route in terms of elevation from point A to point B. It shows that there is a net loss in elevation of approximately 250 ft when traveling from point A to point B over the first leg of the test route. Due to this, the fuel consumption when traveling from point A to B was compared to the consumption when traveling from point B to A, which has a net gain in elevation. The reliance of energy regeneration on gravitational potential energy suggested that direction of travel might impact the results.

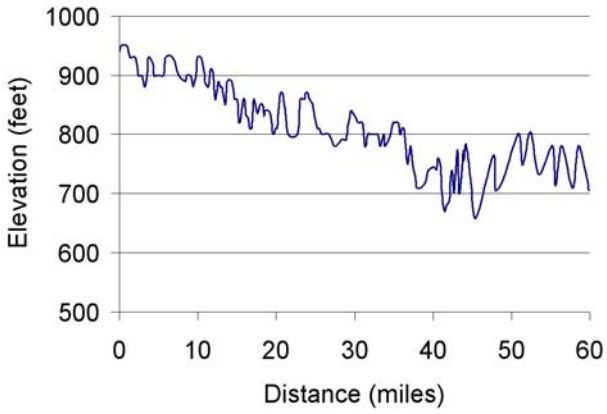

Figure 17 Elevation Plot of One Leg of the Test Route (Point A to Point B)

To look more closely at this, the ECM-calculated fuel rate signal was used to indicate the relative amount of fuel consumed across the different configurations. The data was first normalized for all runs and configurations. Each run was then broken down into 4 sections, each representing one 58-mile leg of the run, with 2 of the legs making up one lap. Figure 18 shows the vehicle speed plot for one lap of the run, covering the same stretch of road in alternating directions. The truck begins at point A and turns around at point B. Each leg was analyzed from the point the truck reached the set speed until demand was cut at the turn-around. This provided the additional benefit of looking at the performance during steady-state operation without having to consider the fuel used while turning around.

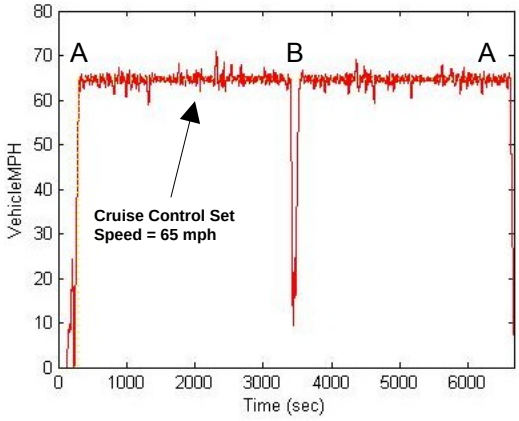

Figure 18 Vehicle Speed Plot for One Lap of Test Route

The chart in Figure 19 summarizes the results of fuel consumption relative to the direction of travel on the route, A to B being the direction resulting in a net loss of elevation or 'downhill', B to A being the opposite, 'uphill'. The data is normalized to the average

This report was prepared with the support of the U.S. Department of Energy, under Award No. DE-FC26-04NT42189. However, any opinions, findings, conclusions, or recommendations expressed herein are those of the author(s) and do not necessarily reflect the views of the DOE.

baseline fuel consumption in both directions. Consistent with the composite test data, both the regenerate-only and propulsion assist configurations provide a fuel consumption benefit. For this route, the regenerate-only configuration provided greater overall improvement than the propulsion assist configuration. This figure highlights the source of the benefit to an additional level of detail.

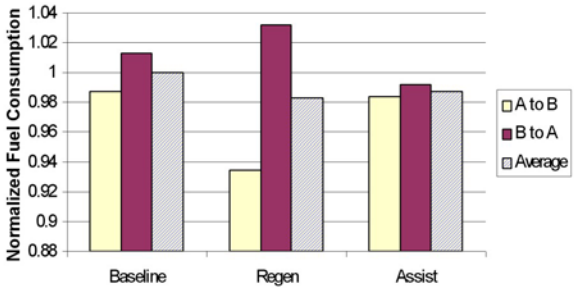

Figure 19 Normalized Fuel Consumption Dependent on Direction and Configuration

The data suggests that in all configurations, more fuel is consumed on the uphill portion of the run than on the downhill, which is consistent with the work energy theorem relative to gravitational potential energy. An interesting result is that the regenerate-only configuration appears to actually increase the fuel consumption on the uphill portion of the run relative to the baseline. The net improvement then comes as a result of the improvement on the downhill portion, which is most likely a result of the reduced amount of regeneration (relative to assist) on the downhill portion leading to increased energy stored in vehicle momentum. On the net uphill portion, when gravity is doing counterproductive work on the vehicle, there is much less energy to be gained over the run. In this case, the regeneration and subsequent slight loss in momentum may be the cause of the increased fuel consumption.

The propulsion assist configuration appears to have achieved a better balance in the fuel consumption between the different directions, with the uphill portion only requiring slightly more fuel than the downhill portion. This averages to a small improvement over the baseline data, however, not as significant an improvement as the downhill portion for the regenerative braking only configuration. Similar to a previous observation, the increased regeneration proved to provide only a small advantage over the baseline. The data shows that in the downhill direction, relative to the regenerative braking only configuration, the propulsion assist configuration is decidedly worse. Conversely, the propulsion assist configuration does provide the best fuel consumption on the uphill portion. These results suggest that further optimization and customization of the controls could provide additional improvements.

Comparison to Original Simulations

Looking at the road profile for the fuel economy testing, the profile was determined to have a maximum grade of 4.05 percent with an average elevation frequency (peak-to-peak) of approximately 3.3 km. Referring back to Table 6, the original simulation data suggests a reduction of fuel consumption greater than 2.3 percent (assuming a increasing trend with respect to a constant 4 percent grade and decreasing elevation frequency). The measured results of a 2.2 percent improvement, while not an exact match for the simulation data, do corroborate the predicted results.

The differences between the measured results and the simulations can be attributed to a combination of differences between the power management algorithms and the hill profiles. The original simulations included a different depth of discharge and SOC limits for the batteries. The simulations also utilized different parameters in the power management strategy such as the range of engine torque where the ISG would assist. Considering the road profiles, the simulations used a sinusoidal profile with no net change in elevation. The hills were uniform in the simulations while the actual road profile for testing had a varying elevation frequency and grade. The simulated numbers themselves show dramatic differences in results with changes in the road profile. The combination of these disparities between the road tests and the initial simulations explain any small differences in the exact magnitude of the gains.

Improvement

Based on the previous results, the AES truck was able to improve the fuel efficiency; however, further analysis of the data showed that there is potential improvement to be had. Areas for potential improvement include further control optimization and profile specific power management.

Changes to the control algorithm for the energy storage system and ISG may provide improvements. For example, the current control algorithm provides 100 percent ISG power when assisting and generating which is essentially a step input of torque to the drivetrain. Changing this to be variable, or a ramp input, maybe provide increased capability when the full power is not needed. This would allow improved management of stored energy and potentially an improvement in fuel economy.

Based on the test data, there is room to optimize and improve the power management on the vehicle. One area identified as being critical to fuel consumption

This report was prepared with the support of the U.S. Department of Energy, under Award No. DE-FC26-04NT42189. However, any opinions, findings, conclusions, or recommendations expressed herein are those of the author(s) and do not necessarily reflect the views of the DOE.

was the road profile. The data showed that even covering the same stretch of road in opposite directions could have dramatic effects on fuel consumption relative to the power management strategy. This result brings up the potential benefit of having a control strategy that will adapt to the road profile by having information on the road ahead of the truck. This could be accomplished by using GPS in real time or loading data files containing a preprogrammed route. Using GPS to actively adapt the control to the approaching road would allow increased flexibility but may not provide the best fuel economy. A realistic limit on the complexity of the controls and range of adaptability may limit the fuel savings. On the other hand, if the truck's route was known, and the controls could be optimized for that specific route, there are potentially even more significant improvements in fuel economy to be had. For example, if there was a large hill approaching and this was known, the truck could store additional energy and operate outside the limits set to optimize the control for a generalized road profile.

Similarly, as the data shows the potential dependence of fuel economy on the direction of travel, using the assist configuration in one direction and the regenerative braking configuration in the opposite direction might provide the greatest benefit.

CONCLUSION

The AES project successfully demonstrated cooling package enhancements and advanced power management strategies for an electrified truck chassis. During 2007, the team completed integration of the electric cooling fan, stainless steel aftercooler, and energy storage system into the MET platform. Component integration enabled thermal performance testing utilizing the newly installed 2007 engine on the chassis dynamometer. Capitalizing on the increased robustness in temperature control offered by the electric components and new cooling module, the team investigated fuel economy improvement opportunities in addition to capability enhancements. The reworked cooling system demonstrated the ability to reduce fuel consumption by 2.7 percent during typical steady state conditions. Furthermore, the ambient capability of the system was increased by more than 6 °C.

Following chassis dynamometer testing, the team performed on-road testing of mild-hybrid operation with the ISG providing regenerative braking and cruise assist. These functions yielded a 2 percent increase in fuel economy during on-road testing. The improvements seen on the chassis dynamometer and during on-road testing are believed to be largely additive because of their natural independence. Chassis dynamometer testing made no allowance for regenerative braking or cruise assist. Current into and out of the energy storage system was held constant at zero during these tests. The ISG was operated only enough to service the power requirements of accessories on the 340 VDC and 12 VDC buses, thus the ISG merely mimicked the operation of a conventional alternator. Conversely, the on-road testing only examined the impact of control algorithms that make use of the ISG and the energy storage system in different manners. On-road testing was conducted during a period of cooler ambient temperatures, leading to lower loads on the cooling module, reducing both radiator flow and fan operation. Per the results shown in Figure 12, significant reductions in fuel consumption are achieved via the utilization of the full AES cooling module. Testing constraints did not permit on-road testing of the elevated top tank temperature; nevertheless, the chassis dynamometer data clearly indicates the gains offered by this change as well. Finally, fuel economy should also profit from further optimization of the control algorithms to better account for route details.

The combination of these factors suggests that the technologies implemented during this program offer the opportunity to improve fuel economy by greater than 4 percent, a substantial savings for long haul applications. Combining these technologies with the MET results suggests savings approaching 10 percent for long haul applications. Previous work in this program suggests that each one percent improvement in fuel economy might equate to approximately $2300 of present value to the operator[1]. Further, collateral benefits such as emission reductions may increase the customer value of an ISG, stepping up acceptance of the technology, while also providing critical fuel savings. As such, the technologies evaluated during this program would not only reduce fuel consumption and emissions, but also do so in a value-added fashion, facilitating adoption through a variety of markets.

[1] Figure based on $2.75/gallon for diesel fuel with 125,000 miles/year on each truck and a 6-year lifespan for each truck.

This report was prepared with the support of the U.S. Department of Energy, under Award No. DE-FC26-04NT42189. However, any opinions, findings, conclusions, or recommendations expressed herein are those of the author(s) and do not necessarily reflect the views of the DOE.

APPENDIX A: PUBLIC RELEASES OF RESULTS

Pointer, W.D., et al., "Applicability of Commercial CFD Tools for Assessment of Heavy Vehicle Aerodynamic Characteristics," in F. Browand, J. Ross, and R. McCallen, eds. *The Aerodynamics of Heavy Vehicles II: Trucks, Buses and Trains*, Berlin:Springer. [in production]

"Advanced Systems for Electrification of Heavy Duty Trucks" (06CV-124) presentation given by Kris W. Johnson on 11/02/2006 at the Society for Automotive Engineers 2006 Commercial Vehicle Engineering Congress & Exhibition.

This report was prepared with the support of the U.S. Department of Energy, under Award No. DE-FC26-04NT42189. However, any opinions, findings, conclusions, or recommendations expressed herein are those of the author(s) and do not necessarily reflect the views of the DOE.

APPENDIX B: INVENTIONS/PATENT APPLICATIONS

INVENTION TITLE	INVENTOR(S)	DATES REPORTED	DOCKET NUMBER APPLICATION NUMBER
INV 1 – File # 05-562 "Switched Capacitor DC Converter"	Chris Hickam	Subject Invention: 10/17/05	S-108,956
INV 2 – File # 05-901 "Powertrain with Powersplit Pump Input and Method of Use Thereof"	Kris W. Johnson Charles E. Rose	Subject Invention: 2/10/05 Elect Title: 10/13/06 Filed in Japan: 5/10/07 Filed in Germany: 4/13/07	S- 109,977 App: 11/485,777 JP 2207-125491 DE 102007017487.1
INV 3 – File # 06-301 "Auxiliary Power Unit for Moving a Vehicle"	Sivaprasad Akasam Kris W. Johnson Matthew D. Johnson Larry M. Slone James Milton Welter	Subject Invention: 4/26/06 Elect Title: 12/19/06	S-110,377
INV 4 – File # 06-397 "Advanced Cooling System Utilizing Electrical Thermostats"	Chris Hickam Timothy Evans Kris W. Johnson Kranthi Kothamachu Larry M. Slone	Subject Invention: 5/8/06	S-112,218

This report was prepared with the support of the U.S. Department of Energy, under Award No. DE-FC26-04NT42189. However, any opinions, findings, conclusions, or recommendations expressed herein are those of the author(s) and do not necessarily reflect the views of the DOE.